Effect of the Thermal Histories on Case II Sorption Kinetics: Test of a Kinetic Theory for Swelling

G. C. SARTI,* A. APICELLA, and C. DE NOTARISTEFANI,† *Istituto di Principi di Ingegneria Chimica, Facoltá di Ingegneria, Universitá degli Studi di Napoli, Piazzale Tecchio 80125, Naploli, Italy*

Synopsis

Case II sorption kinetics have been analyzed for PS–*n*-hexane systems. Samples of polystyrene characterized by several different annealing histories were used. For all thermal histories, the *n*-hexane sorption kinetics at several temperatures were measured, as well as some relevant mechanical properties of the glassy matrix, e.g., density and initial stress for crazing. The main influence of the thermal history is to appreciably alter the initial stress for crazing σ_c, as well as the swelling kinetics. The σ_c curve vs. annealing time is seen to go through a minimum which is paralleled, at 40°C, by a maximum in the swelling kinetics. The independent mechanical and sorption data obtained were compared with a recently proposed [G. C. Sarti, *Polymer*, **20**, 827 (1979); G. C. Sarti and A. Apicella, *Polymer*, **21**, 1031 (1980)] theory for Case II kinetics, which is shown to be particularly suitable to describe the observed behavior.

INTRODUCTION

It is widely known that the sorption of solvent molecules in glassy polymers gives rise to a large variety of behaviors.[1–22] The physical phenomena that simultaneously occur are dissolution, diffusion, swelling, and relaxation, together with deformation and stress buildup in the matrix. A comprehensive mathematical description accounting for the manifold phenomenology observed does not seem to be achieved as yet, although several mathematical models have been proposed so far.[23–38]

In the case of polystyrene matrix, the kinetics of the swelling process, occurring at the moving front, is suitably described through the localized swelling model proposed in Ref. 33. According to that model, the effects of the penetrant is lumped into an osmotic tension π which depends upon the polymer–solvent pair and on the gel composition at the moving front. The velocity of the advancing swelling front is then obtained by using the mechanical crazing kinetics under an external load, in which the tensile applied stress is suitably substituted by the osmotic tension. In Refs. 33 and 35 the model was compared with different literature data from which, however, only a qualitative test can be obtained, since the data refer to different polystyrenes, treated with different thermomechanical histories. Our aim here is to provide for experimental data on which a quantitative test for the theory could be based. We will analyze independently both the

* Present address: Istituto di Impianti Chimici, Facoltá di Ingegneria, Universitá di Bologna, Viale Risorgimento 2, 40136 Bologna, Italy.

† Present address: TEMA S.p.A., Via Aldo Moro 38, Bologna, Italy.

Journal of Applied Polymer Science, Vol. 29, 4145–4159 (1984)
 CCC 0021-8995/84/124145-15$04.00

relevant mechanical properties of the polymer matrix and the sorption behaviour shown by deeping it in liquid *n*-hexane.

The attention will be focused in particular on the influence of the prior thermal history and of the present temperature. Normal hexane was the only penetrant considered insofar as the behaviour of other *n*-alkanes does not change the mechanical parameters of the model but only the particular value of the osmotic stress.[33,35]

Although some nonmonotonous behaviors are observed with increasing the annealing time, the localized swelling model proves to be particularly adequate to describe the observed Case II kinetics.

EXPERIMENTAL

Powder polystyrene was used, supplied by Rapra Co., $M_w = 200{,}000$, $T_g = 100$°C. Polymer sheets were obtained in a Wabash hydraulic mould at 150°C and at 50 MPa approximately. In order to erase the internal stress dishomogeneity generated during the molding process, all samples were first annealed for 3 h at 140°C and then air-quenched. After quenching, some samples were used as such and, the others were subject to several subsequent annealing histories, by keeping the samples in the oven either at 70 or at 90°C for different annealing times. In the oven the temperature was controlled to within 1°C and a vacuum of 700 mm Hg was maintained.

After the different thermal histories were completed, a mechanical characterization of the samples was obtained by measuring (a) the sample density at 20°C and (b) the threshold tensile stress for crazing in air, at 20, 40, and 60°C.

Density measurements were performed through a gradient column working at 20.0 $\pm$ 0.1°C, obtained by using NaCl solutions with a gradient of 3.0×10^{-5} g/cm^3 cm; RPE grade NaCl was used for that purpose, supplied by Carlo Erba. The relative heights of the tested samples were measured by a cathetometer sensitive to 0.05 mm; the column was sensitive to density differences of the order of 10^{-5} g/cm^3. All the samples used found their equilibrium position within a 30-cm span.

The critical stress for crazing in air was also measured; such quantity plays an important role in connection with both polymer characterization and sorption kinetics. Tensile tests were performed by using an Instron 1102 apparatus at low deformation rate ($\dot{\epsilon} = 1.67 \times 10^{-5}$ s^{-1}); the deformations were measured directly through a strain gange.

The tensile tests were performed at 20, 40, and 60°C by using an Instron thermostatic chamber. The onset of crazes was visually observed directly in the sample surfaces.

Each data point results from 10 equivalent runs so that the confidence interval of 95% was reliably evaluated.

Sorption experiments were performed by deeping the polymer samples into liquid *n*-hexane, RPE grade, supplied by Carlo Erba S.p.A. The temperature of the liquid penetrant was controlled to within 0.1°C by using a thermostatic units; several experimental temperatures were used, ranging from 20 to 60°C. Two different series of sorption experiments were considered in order to measure both weight gain and penetration depth vs. time.

The experiments ended when an asymptotic weight uptake was obtained, which was dealt with as equilibrium value, although it is not in general the true thermodynamic equilibrium value.[39]

The weight uptake was measured periodically according to the following procedure: The samples were taken out of the bath and quenched at −20°C in order to stop solvent penetration and prevent its evaporation; the outer surface was then dryed, and the samples were weighted by using a Galileo Sartorius balance, reading 0.05 mg. Penetration depths were also measured by using an optical microscope Stereoscan with incident light. The thickness δ_0 of the sample was initially measured. The position of the moving swelling front was recorded by measuring the thickness of the glassy core δ and the depth λ of the swollen layer, along the direction perpendicular to the major surfaces of the sample. Prior to the microscope readings, the sample internal surface to be observed was prepared by removing the swollen polymer from the upper edges; first a microtome and then an abrasive treatment were used. The measurements performed are to within 0.01 mm precision. For the very initial stages the more reliable readings are given by the penetration depth λ; the initial core thickness δ was obtained by making use of the observation that the ratio $2\lambda/(\delta_0 - \delta)$ remains a constant, equal to 1.10, during a significant portion of the sorption process, particularly at short times of sorption.

RESULTS

Density measurements follow the expectation based on the volume relaxation phenomena.[40] The lowest density was observed in quenched samples ($\rho = 1.036$ g/cm^3) and the higher densities were obtained for the longer annealing times. Figure 1 represents the density difference between annealed and quenched samples vs. annealing time; at long times both curves at 70 and 90°C coincide and seem to tend to the same density difference of 1×10^{-3} g/cm^3. Through Figure 1 a quantitative representation is obtained

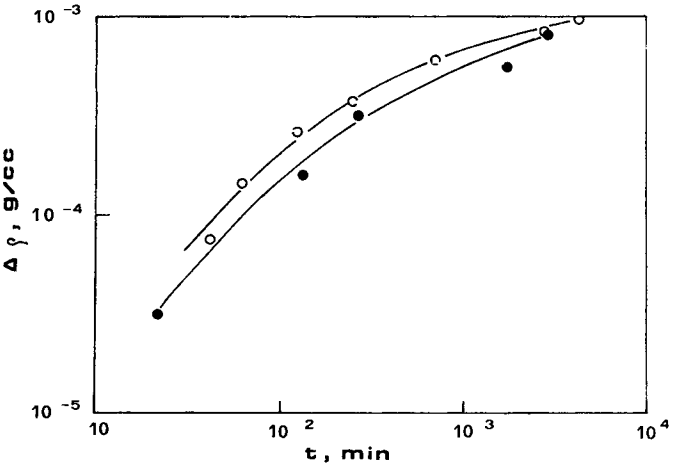

Fig. 1. Density difference between annealed and quenched samples versus annealing time: (●) 70°C; (○) 90°C.

of the relative out of equilibrium which is trapped into the glassy matrix after the thermal history considered.

In Figure 2 the critical tensile stress for craze formation is reported vs. the annealing time at 70°C, at the test temperatures of 20, 40, and 60°C, respectively. As is apparent, σ_c is a quantity rather sensitive to the thermal history and undergoes changes up to 50% with different annealings. Unexpectedly, a nonmonotonous behavior is observed vs. the annealing time. On the bases of the observed free volume decrease with increasing the duration of the thermal treatment, a parallel increase in the σ_c value was expected, while, instead, at all the tested temperatures an initial σ_c decrease was observed followed by a subsequent increase, with increasing the annealing time. We are here interested in observing the mechanical properties of the samples used, more than in finding a definite explanation for such behavior. A possible explanation, however, could be found by considering that, in quenched samples, the outer layers glassify prior to the internal core and thus are left under a compression which relaxes during the annealing; as a consequence a higher external load must be initially applied in order to obtain crazing. Another possible explanation can be found in connection with the fact that the properties of the glass should not be related to a single state variable (i.e., density) but to at least two state quantities.[41]

Table I summarizes the measured mechanical properties for the samples annealed at 70°C. The values of σ_c, relative to the same annealing time, change almost linearly with temperature and vanish at the glass transition, as is shown in Figure 3: ($\sigma_c = A(T_g - T)$, where the slopes A for the 0, 4, and 72 h annealings, are 0.239, 0.210, and 0.273 MPa/°C, respectively. The above behavior has been observed by using the samples soon after their thermal history was completed. Preliminary experiments performed on samples kept at room temperature for about 10 days after their treatment in the oven showed that the dwelling time at room temperature played the role of a subsequent thermal history which masked the effects produced by the prior annealing and rather scattered data were obtained by plotting σ_c vs. the time elapsed in the oven.

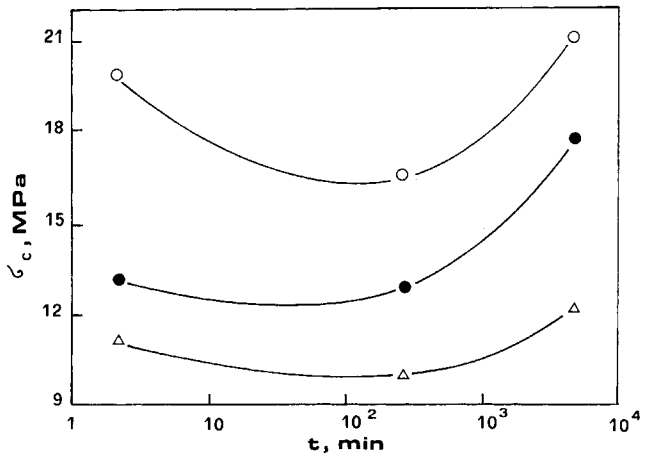

Fig. 2. Critical tensile stress for craze formation versus annealing time at 70°C, at 20°C (○), 40°C (●), and 60°C (△).

TABLE I
Mechanical Properties of Annealed Samples

T (°C) of the test	t anneal. (h)	σ_c (MPa)	ϵ_c	σ_b (MPa)	ϵ_b	E (MPa)
20	0	19.8 ± 1.5	7×10^{-3}	33.0	1.3×10^{-2}	3500
20	4	16.5 ± 1.3	7×10^{-3}	29.0	9.5×10^{-3}	3200
20	72	21.0 ± 1.8	7.5×10^{-3}	34.0	4.5×10^{-3}	2900
40	0	13.0 ± 1.1	4×10^{-3}	27.0	1×10^{-2}	3000
40	4	12.7 ± 1.0	8×10^{-3}	26.5	1.5×10^{-2}	2700
40	72	17.6 ± 1.2	6.5×10^{-3}	29.0	1.1×10^{-2}	2700
60	0	11.0 ± 0.9	8×10^{-3}	21.0	1.5×10^{-2}	2200
60	4	9.8 ± 0.7	8.5×10^{-3}	20.0	2×10^{-2}	1900
60	72	12.0 ± 0.9	9×10^{-3}	21.5	2.1×10^{-2}	2000

Sorption experiments have been performed at the temperatures of 30–60°C, with a scan of 10°C. Samples were annealed at 70°C for different periods of time ranging from 10 min to 3 days. In Figures 4(a)–(d) we report time vs. the data of the penetration depth S_e, measured with respect to the position of the initial external surface of the unpenetrated sample. For sake of simplicity only data relative to three thermal histories have been reported. In Figures 5 the sorption data at different temperatures are reported, for samples characterized by the same annealing treatments (4 and 72 h at 70°C, respectively).

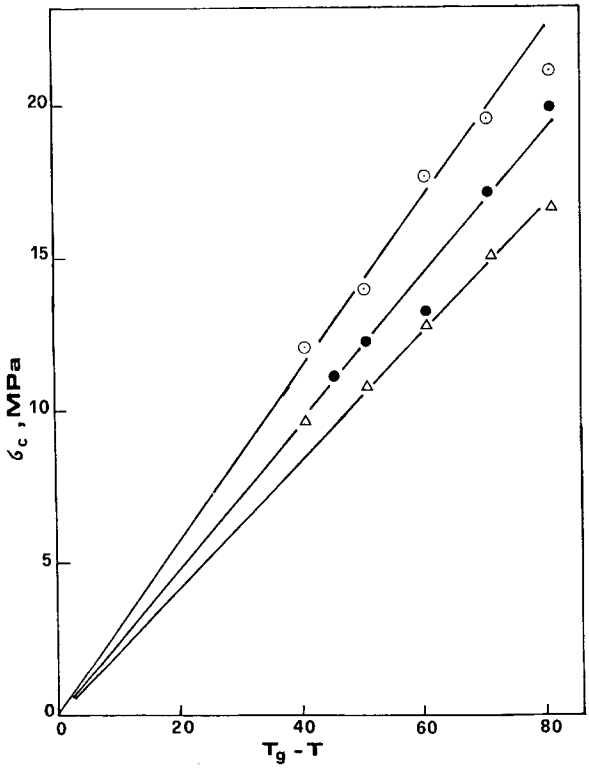

Fig. 3. Critical tensile stress for craze formation versus present temperature, for quenched samples (○) and annealed 4 h (▲) and 72 h (●) samples.

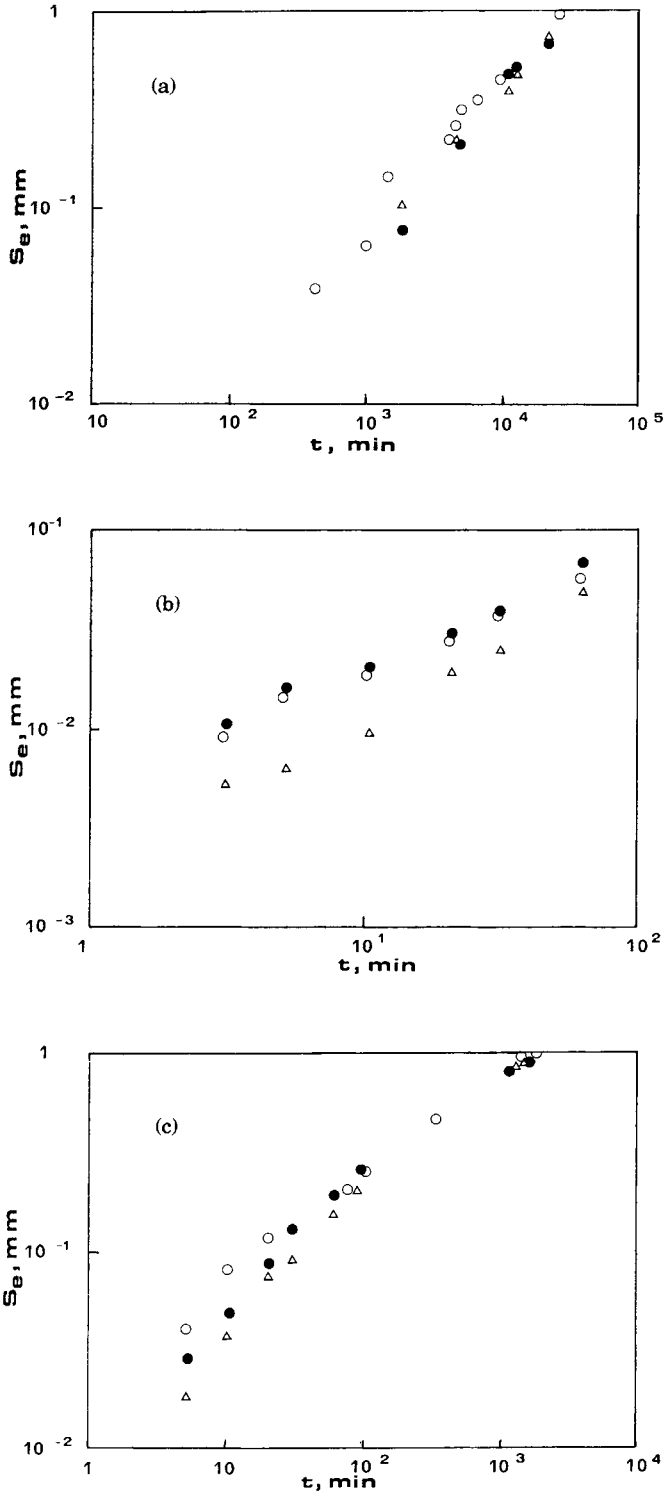

Fig. 4. Penetration depth vs. time for different thermal histories: quenched samples (○), annealed 4 h (●) and annealed 72 h (△): (a) 30°C; (b) 40°C; (c) 50°C; (d) 60°C.

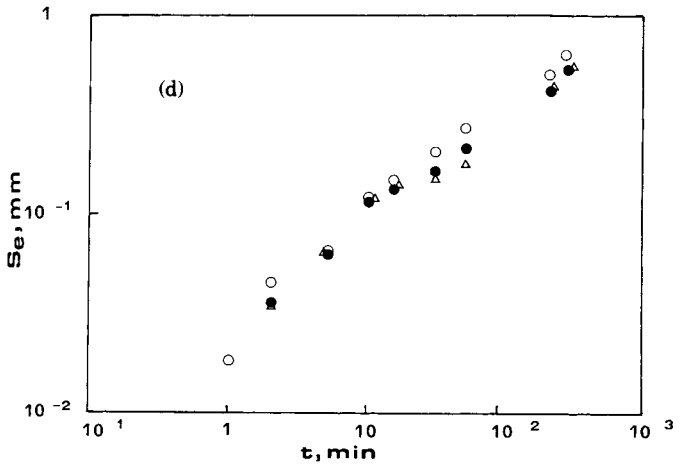

Fig. 4. *(Continued from previous page.)*

The value of the penetration rate associated with the limiting Case II sorption has been taken during the initial stages of the test. The rate of penetration of the advancing front, in fact, is progressively reduced as a consequence of the diffusion resistence developed in the swollen region. The curves of Figure 5 clearly indicate that the sorption is initially controlled by relaxation at all the temperatures investigated (slope equal to 1 according to Case II), while it is governed by the diffusion in the swollen polymer when a sufficiently thick layer is developped (slope equal to 0.5).

The values of the penetration rates are reported in Table II vs. annealing time and sorption temperature. All reported data come from at least three experimental runs. It is apparent from Figures 4 that the differences in the sorption behavior due to different thermal histories are more significant at the initial stages of sorption while at longer times the various isothermal curves become closer to each other. It must be observed in this respect that,

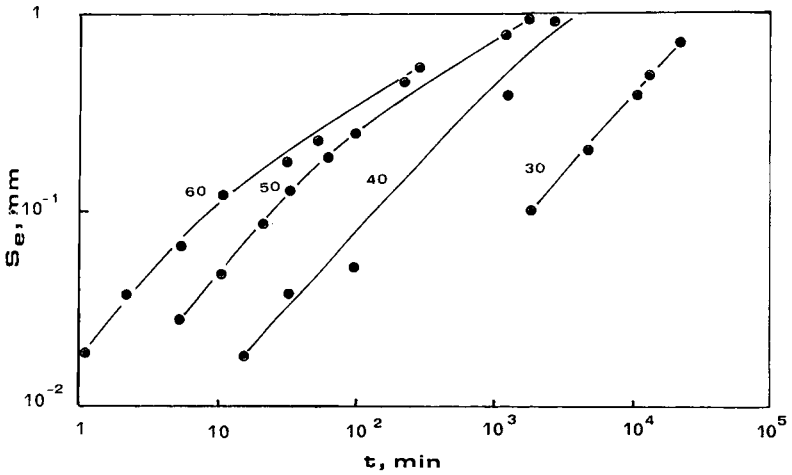

Fig. 5. Penetration depth vs. time for the same thermal history (annealing at 70°C, 4 h) at 30°C (△), 40°C (○), 50°C (□), and 60°C (×).

TABLE II
Initial Swelling Rate vs. Annealing Time and Sorption Temperature[a]

	t (h)		
T (°C)	0	4	72
30	9.5×10^{-5}	6.10×10^{-5}	4.5×10^{-5}
40	8.7×10^{-4}	2.4×10^{-3}	1.8×10^{-3}
50	7.2×10^{-3}	5.5×10^{-3}	3.6×10^{-3}
60	1.8×10^{-2}	1.8×10^{-2}	1.8×10^{-2}

[a] Initial penetration rate in mm/min.

although during the sorption samples undergo a simultaneous annealing treatment, its influence becomes significant only for times not considered for the calculation of the sorption rates.

For the same prior thermal history, an increase in the sorption temperature results in a significant increase in the velocity of the advancing front; this observation is consistent with the expectations based on the Eyring activated process idea and with the high activation energy which must be associated with the Case II kinetics (e.g., Ref. 17).

On the other hand, an increase in the annealing time was expected to result in a decrease in the isothermal sorption rate, in view of the simultaneous decrease in the free volume frozen into the glass. Unexpectedly, the latter prediction is not general. In fact, although it is consistent with the sorption data at 30°C and 50°C showing a monotonous decrease with increasing the annealing time, that expectation is, on the contrary, violated by the sorption data at 40°C. At the latter temperature a relative maximum in the sorption rate is observed when the annealing time at 70°C increases from 2 to 72 h.

The sorption experiments were performed up to an apparent equilibrium was reached. Actually, after sorption intervals as long as five times the time needed for the disappearance of the glassy core, the final situation reached showed small regular oscillations in the weight uptake; the amplitude is in the order of 10% of the average weight uptake and is slightly decreasing with dwelling time. Such behavior is well reproducible. The average value for the weight uptake was considered as the equilibrium value, in spite of the many words of caution cleverly illustrated by Enscore et al.[39]

Consistently, the equilibrium values thus measured were found to be independent of the prior thermal history experienced by the polymer matrix. Such values, shown in Table III, are rather temperature-independent apart from the data at higher temperatures at which higher values were

TABLE III
Equilibrium Volume Fractions $\phi_{1,eq}$, χ Parameters, and Osmotic Tension Contributions π_{eq}, π^E

T (°C)	20	30	40	50	60
ϕ_{eq}	0.18	0.18	0.17	0.23	0.20
χ_1	1.0833	1.058	1.035	1.014	0.994
π (MPa)	3.24	3.37	3.50	3.63	3.75
π^E (MPa)	9.29	8.12	6.96	5.79	4.60
π (MPa)	12.53	11.49	10.46	9.42	8.35

obtained. It is worth noticing that at higher temperatures higher swellings were also obtained which eventually result in the simultaneous formation of microcavities, in which the penetrant could be just stored as such instead of being uniformly dissolved in the polymer matrix. Such phenomena are known to occur in other polymeric systems.[42]

Discussion and Testing of the Theoretical Model

As previously anticipated, the data obtained have been analyzed by using the localized swelling theory as recently proposed in Refs. 33 and 35. For sake of simplicity it is here convenient to briefly recall the most significant features of the theory.

(i) First of all, the influence of the particular penetrant on the polymer matrix is lumped into an osmotic tensile stress π; this idea, first introduced in Ref. 33, has been recently used in a nonlocalized model.[38]

(ii) The swelling process is localized at the moving interface which separates the glassy unpenetrated matrix from the swollen penetrated polymer.

(iii) The velocity of the advancing swelling front is well represented by the kinetics of crazing under external tensile load in a dry environment, after the osmotic tensile stress has been suitably used for the applied stress.

As already discussed in Refs. 31, 33, and 35, the above assumptions represent a very simplified picture of the process in many respects, e.g., the plastification effects due to the particular solvent ahead the moving interface are neglected; in addition, the swelling process is not always completed in the polymer soon after the glassy-swollen transition but continues according to the polymer relaxation spectrum.

The above assumptions refer to the kinetics of the advancing front; obviously, the entire mass transfer process is completed when diffusion is accounted for in both swollen layer and glassy core. Our present aim, nonetheless, is to test whether or not the localized swelling model well represents the swelling kinetics observed; thus particularly significant will be the velocity data at short times since will refer to a situation in which no concentration gradient is present in the swollen layer. The diffusion in the glassy core will be neglected, as is usually well accepted in Case II transport.

The above model can be quantitatively applied to polystyrene–*n*-hexane systems by using the following crazing kinetics for crazing in dry air[43]:

$$v = k(\sigma - \sigma_c) \tag{1}$$

where the kinetic constant k is taken to be only temperature-dependent; from data of Maxwell and Rahm[44] we have

$$k = k_0 \exp(-E/RT),\ k_0 = 1.92 \times 10^{20}\ \text{cm/s},\quad E = 40{,}000\ \text{cal/mol} \tag{2}$$

The osmotic tension π was first introduced through the polymer partial molar quantities in Ref. 33, and is not to be confused with the more common osmotic pressure used for dilute polymer solutions; one has

$$\pi = \frac{\mu_2^0 - \mu_2}{V_2} \tag{3}$$

Such quantity can be split into the sum of an equilibrium (π_{eq}) and an out of equilibrium (π^E) contributions. The former can be calculated by simply using the Flory–Huggins constitutive equation which, in the absence of crosslinks, leads to

$$\pi_{eq} = \frac{\mu^0_{2,eq} - \mu_2}{V_2} = \frac{RT}{V_1}\left[\phi_1 - \chi_1\phi_1^2 - \frac{1}{x}\ln(1 - \phi_1)\right] \tag{4}$$

where ϕ_1 represents the penetrant volume fraction at the swollen interface and V_1 its molar volume; x indicates the degree of polymerization, and χ_1 is the Flory interaction parameter.

In the isotropic case here considered, the out-of-equilibrium contribution π^E is associated with the excess volume frozen into the glassy polymer. By using an S-ring type constitutive equation, according to the procedure used in Ref. 35, one obtains

$$\pi^E = \frac{\mu_2^0 - \mu^0_{2,eq}}{V_2} = \frac{P^*}{\rho^{*2}}\rho(\rho_{eq} - \rho) \tag{5}$$

where ρ and ρ_{eq} are the pure polymer densities at temperature T in the present glassy state and in the hypothetical equilibrium state respectively. The critical state quantities P^* and ρ^* in the case of polystyrene are given the following values[45]:

$$\begin{aligned} P^* &= 348.5 \text{ MPa} \\ \rho^* &= 1.105 \text{ g/cm}^3 \end{aligned} \tag{6}$$

By using the above expressions the osmotic tension is thus obtained as

$$\pi = \frac{RT}{V_1}\left[\phi_1 - \chi_1\phi_1^2 - \frac{1}{x}\ln(1 - \phi_1)\right] + \frac{P^*}{\rho^{*2}}\rho\,(\rho_{eq} - \rho) \tag{7}$$

According to the model, the kinetics of the advancing front are given by

$$V = k(a\pi - \sigma_c) \tag{8}$$

where k and σ_c are the same quantities appearing in eq. (1), and a is an equivalence factor which accounts for the fact that π is an isotropic tension while the stress σ appearing in eq. (1) is a uniaxial tensile stress. According to Andrews and Levy's analysis,[46] the equivalance factor a ranges between 1 and 3; more precisely, it is $\pi = \sigma/3$, i.e., $a = 3$, for spherically shaped crazes, and it is $\pi = \sigma$, i.e., $a = 1$, for crazes in which the longitudinal dimension is much larger then the transversal one.

Equation (8) represents one of the basic equations of our model; through it, the factor a enters the problem as a parameter associated with the shape of the crazelike microvoids which are formed at the swelling front; the equivalence factor is to be considered a property of the plasticized glassy matrix at the swelling front.

A suitable test for the localized swelling model can be performed as follows. Consider the sorption process at short times; the swollen region is practically at the uniform equilibrium concentration, which was measured; in this case π can be calculated through eqs. (4), (5), and (7). The initial swelling rate v_0 and the critical stress for crazing σ_c have been independently measured. By considering K a function of temperature only, as given by eqs. (2) and (8) is then used to calculate what value of the factor a is needed in order to fit the independently measured data on swelling rate and stress for crazing. The same calculations, performed for all the samples treated by the several thermal histories considered, provide for the set of data on which the present test is based.

The osmotic tension contributions, needed for the test, are reported in Table III, together with the equilibrium volume fraction of n-hexane and with the corresponding Flory interaction parameter χ_1. It must be observed that one only value is reported for π^E at a given temperature; actually, the annealing treatments considered change the polymer density and, thus, also π^E in view of eq. (5). In the present case, nonetheless, the maximum density difference of 10^{-3} g/cm^3 corresponds to minor differences in π^E infacts

$$\Delta\pi^E \sim \frac{P^*}{\rho^{*2}} \rho_0 \Delta\rho \sim \frac{348.5}{(1.105)^2} 1.036 \times 10^{-3} \sim 0.3 \text{ MPa}$$

From the above estimate, in view also of the σ_c data reported in Figure 2, 10–20 MPa, the conclusion is drawn that the main influence of the thermal histories here applied is to appreciably alter the values of the threshold stress σ_c, keeping almost constant the osmotic tension.

The test of the localized swelling model is summarized in Table IV, in which the values of parameter a are reported, calculated from eq. (8) by using the swelling rates experimentally observed at different temperatures and different thermal histories. It is also interesting to simultaneously observe the relative role played by the other physical quantities entering the model. As is apparent, several different calculations have been performed.

First of all the same procedure as in Ref. 33 is considered; i.e., use is made of the literature data for both k, reported in Ref. 44, and σ_c, reported in Ref. 43, and in addition only the equilibrium contribution is considered for π (Table IV, column 1); the factor a thus results both temperature and history dependent and, in addition, ranges between 2.4 and 6.3 instead of being $1 \leqslant a \leqslant 3$. However, if π is calculated as $(\pi_{eq} + \pi^E)$, and the same literature data for σ_c and k are used as previously (procedure followed in Ref. 35), the temperature dependence of a is appreciably reduced to the range between 1.1 and 2.2 (see Table IV, column 2), but both a temperature and a history dependence are observed, contrary to the physical meaning of such a parameter.

On the contrary, when the experimentally observed values for σ_c are used in the calculations, the equivalence factor a results independent of the prior thermal history undergone by the polymer matrix (Table IV, columns 3 and 4). Therefore, the significant conclusion is drawn that the annealing processes are essentially accounted for by the particular σ_c values.

TABLE IV
Temperature and Annealing Time Dependence of Parameter a, Calculated through Eq. (8) by Using Our Penetration Rate Data and Indicated Data of π, σ_c, and k

	$\pi = \pi_{eq}$ σ_c, from Ref. 43 k, from Ref. 44			$\pi = \pi_{eq} + \pi^E$ σ_c, from Ref. 43 k, from Ref. 44			$\pi = \pi_{eq}$ σ_c, present data k, from Ref. 44			$\pi = \pi_{eq} + \pi^E$ σ_c, present data k, from Ref. 44			$\pi = \pi_{eq} + \pi^E$ σ_c, present data k, from eq. (8)		
	t (h)			t (h)			t (h)			t (h)			t (h)		
T (°C)	0	4	72	0	4	72	0	4	72	0	4	72	0	4	72
20	6.3	6.3	5.2	1.6	1.6	1.3	8.5	7.8	8.3	2.2	2.0	2.1	2.0	1.8	2.0
30	4.9	4.3	4.0	1.4	1.3	1.2	6.8	5.5	6.6	2.0	1.7	1.9	1.8	1.5	1.8
40	6.4	6.5	4.8	2.1	2.2	1.6	7.9	7.6	6.9	2.6	2.5	2.3	2.1	2.0	2.0
50	4.1	3.6	3.1	1.6	1.4	1.2	5.3	4.5	4.8	2.1	1.7	1.9	1.8	1.5	1.7
60	2.4	2.4	2.4	1.1	1.1	1.1	3.3	3.0	3.7	1.5	1.4	1.7	1.8	1.7	1.8

By comparing the data in Table IV, column 3, in which $\pi = \pi_{eq}$ only, with the data reported in Table IV, column 4, in which $\pi = (\pi_{eq} + \pi^E)$, the particular role played by the out of equilibrium term π^E is apparent; in fact, by using only π_{eq} (Table IV, column 3) the parameter a remains temperature-dependent while is history-independent; when also π^E is used (Table IV, column 4) the temperature dependence also disappears: in such case the parameter a ranges between 1.4 and 2.6 with average value $a = 2.0$ and variance $\beta = 0.12$.

The latter result seems rather satisfactory also in view of the fact that the kinetic constant used in the calculations, k, is taken from the data reported in the literature and not directly measured. It can be seen, for instance, that a better fitting of our data can be obtained by using the activation energy for the kinetic constant of solvent penetration, 40.7 kcal/mol, and turning the preexponential factor to $k_0 = 9.77 \times 10^{20}$ cm/s; in that case the values reported in Table IV, column 5, are obtained in which the average value of a with the confidence interval of 95% is given by $a = 1.82 \pm 0.07$. The latter result actually shows that the analogy between swelling and crazing, on which the model used is based, holds true for the systems considered.

CONCLUSIONS

The sorption and mechanical experimental data show, in addition to the effects of temperature, the particular influence of the thermal histories, on the behavior of polystyrene matrix.

With increasing the annealing time up to 72 h at 70°C the isothermal experiments show that: (i) Density regularly increases, showing, however, only minor changes in the absolute value, 0.001 g/cm^3 at most; (ii) the critical threshold stress for crazing on the contrary shows an initial decrease followed by a subsequent increase, with a minimum value for annealings lasting around 4 hours; such minimum value is more pronounced for lower testing temperatures; (iii) with increasing the annealing time, the initial velocity of the swelling front due to *n*-hexane sorption decreases at 30 and 50°C while it shows a relative maximum at 40°C; at 60°C, on the contrary, no appreciable change is observed. The velocity changes due to annealing treatments can be highly significant and can also produce an order of magnitude variation.

The two set of mechanical and sorption data here obtained proved to be highly consistent with the localized swelling model first proposed in Ref. 33, which, in the case of polystyrene matrix, leads to the expression for the velocity of the swelling front given in eq. (8).

According to the data, the main influence of the thermal histories is here obtained through the appreciable changes of the threshold stress σ_c; in principle, however, thermal histories can be considered in which appreciable density variations are produced, thus resulting also in osmotic tension changes. The osmotic tension π accounts for the amount of penetrant present at the interface in the swollen region through the equilibrium contribution π_{eq} given by eq. (4). In addition, π also takes into account the excess free volume frozen into the glass through the out of equilibrium contribution

π^E, given by eq. (5); the latter contribution proves to be linearly increasing with decreasing the temperature below the glass transition.

The kinetic constant k results to be a function of temperature only, obeying an Arrhenius type law with an activation energy of 40.7 kcal/mol. Finally, the parameter a is constant for all temperatures and thermal histories, equal to 1.8. Physically, a represents the equivalence factor which gives the uniaxial normal stress component σ, perpendicular to the direction of crazing, due to the pressure π inside the crazed material. The value here reported, 1.8, is consistent with Andrews and Levy analysis,[46] which wants $1 \leqslant a \leqslant 3$.

It is worth observing that the model well describes the experimental data, although the latter show some unexpected nonmonotonous behaviors with increasing the annealing time.

Our main attention has been focused on the kinetic law for the advancing front since it represents the most characteristic feature of the localized swelling model. Obviously, the entire mass transfer process is described by the moving boundary problem in which the diffusion equation is solved in the swollen layer and also, possibly, in the glassy region; eq. (8) is then used as evolution equation for the moving boundary. The latter procedure was already analyzed elsewhere.[34,36,37]

A nonlocalized but distributed swelling process has been recently analyzed[38] based on an osmotic tension idea analogous to the one used here and in Ref. 33; albeit the latter is more general in principle, there is no need for it in the systems analyzed in the present work. The Case II sorption behavior shown in PS–*n*-alkane systems is well described by the localized swelling model in which the analogy between swelling and crazing is used.

Useful discussions with Professors H. B. Hopfenberg and W. J. Koros are gratefully acknowledged. This work was partly supported by CNR Grant No. CT 80.00820.11/115.

References

1. G. S. Park, *J. Polym. Sci.*, **11**, 97 (1953).
2. E. Bagley and F. A. Long, *J. Am. Chem. Soc.*, **77**, 2172 (1955).
3. A. C. Newns, *Trans. Faraday Soc.*, **52**, 1533 (1956).
4. F. A. Long and I. Watt, *J. Polym. Sci.*, **21**, 554 (1956).
5. R. M. Barrer, J. A. Barrie, and J. Slater, *J. Polym. Sci.*, **23**, 315 (1957).
6. A. Kishimoto, H. Fujita, H. Odani, M. Kurata, and M. Tamura, *J. Phys. Chem.*, **64**, 594 (1960).
7. A. S. Michaels, H. J. Bixler, and H. B. Hopfenberg, *J. Appl. Polym. Sci.*, **12**, 991 (1968).
8. H. B. Hopfenberg, R. H. Holley, and V. T. Stannet, *Polym. Eng. Sci.* **9**, 242 (1969).
9. H. B. Hopfenberg, *Membrane Science and Technology*, J. Flinn, Ed., Plenum, New York, 1970, p. 16.
10. F. A. Long and D. Richman, *J. Am. Chem. Soc.*, **77**, 2172 (1955).
11. B. R. Baird, H. B. Hopfenberg, and V. T. Stannett, *Polym. Eng. Sci.*, **11**, 274 (1971).
12. C. H. M. Jacques, H. B. Hopfenberg and V. T. Stannett, *Polym. Eng. Sci.*, **13**, 81 (1973).
13. C. H. M. Jacques and H. B. Hopfenberg, *Polym. Eng. Sci.*, **14**, 449 (1974).
14. C. H. M. Jacques, H. B. Hopfenberg, and V. T. Stannett, "Super Case II Transport of Organic Vapors in Glassy Polymers," in *Permeability of Plastic Films*, H. B. Hopfenberg, Ed., Plenum, New York, 1974.
15. H. B. Hopfenberg, V. T. Stannett, and G. M. Folk, *Polym. Eng. Sci.*, **15**, 261 (1975).
16. H. B. Hopfenberg, L. Nicolais, and E. Drioli, *Polymer*, **17**, 195 (1976).
17. L. Nicolais, E. Drioli, H. B. Hopfenberg, and D. Tidone, *Polymer*, **18**, 1137 (1977).

18. L. Nicolais, E. Drioli, H. B. Hopfenberg, and G. Caricati, *J. Membr. Sci.*, **3**, 231 (1978).
19. N. Thomas and A. H. Windle, *Polymer*, **18**, 1195 (1977).
20. N. Thomas and A. H. Windle, *J. Membr. Sci.*, **3**, 337 (1978).
21. N. Thomas and A. H. Windle, *Polymer*, **19**, 255 (1978).
22. A. Sfirakis and C. E. Rogers, *Polym. Eng. Sci.*, **21**, 542 (1981).
23. H. L. Frisch, T. T. Wang, and T. K. Kwei, *J. Polym. Sci., A-2*, **7**, 879 (1969).
24. T. T. Wang, T. K. Kwei, and H. L. Frisch, *J. Polym. Sci., A-2*, **7**, 2019 (1969).
25. J. Crank, *J. Polym. Sci.*, **11**, 151 (1953).
26. J. Crank, *The Mathematics of Diffusion*, Clarendon, Oxford, 1975.
27. J. Crank and G. S. Park, *Diffusion in Polymers*, Academic, New York, 1968.
28. J. L. Duda and J. S. Vrentas, *J. Polym. Sci., A-2*, **6**, 675 (1968).
29. A. Peterlin, *Makromol. Chem.*, **124**, 136 (1969).
30. J. H. Petropoulos and Roussis, *J. Membr. Sci.*, **3**, 343 (1978).
31. G. Astarita and G. C. Sarti, *Polym. Eng. Sci.*, **18**, 388 (1978).
32. A. R. Berens and H. B. Hopfenberg, *Polymer*, **19**, 489 (1978).
33. G. C. Sarti, *Polymer*, **20**, 827 (1979).
34. G. Astarita and S. Joshi, *J. Membr. Sci.*, **4**, 165 (1978).
35. G. C. Sarti and A. Apicella, *Polymer*, **21**, 1031 (1980).
36. C. Gostoli and G. C. Sarti, *Chem. Eng. Comm.*, **21**, 67 (1983).
37. C. Gostoli and G. C. Sarti, *Polym. Eng. Sci.*, **22**, 1018 (1982).
38. N. L. Thomas and A. H. Windle, *Polymer*, **23**, 529 (1982).
39. D. J. Enscore, H. B. Hopfenberg, V. T. Stannett, and A. R. Berens, *Polymer*, **18**, 1105 (1977).
40. A. J. Kovacs, *Trans. Soc. Rheol.*, **5**, 285 (1961).
41. A. J. Kovacs, J. M. Hutchinson, and J. J. Aklonis, in *The Structure of Non-Crystalline Materials*, P. H. Gaskell, Ed., Taylor and Francis, 1977, pp. 153ff.
42. C. Carfagna, A. Apicella, E. Drioli, H. B. Hopfenberg, E. Martuscelli, and L. Nicolais, *Polymer Blends—Processing Morphology and Properties*, E. Martuscelli et al., Eds., Plenum, New York, 1980.
43. J. A. Sauer and C. C. Hsiao, *Trans. ASME*, **75**, 895 (1953).
44. B. Maxwell and L. F. Rahm, *IEC*, **41**, 1988 (1949).
45. J. C. Sanchez and R. H. Lacombe, *J. Polym. Sci., Polym. Lett. Ed.*, **15**, 71 (1977).
46. E. H. Andrews and G. M. Levy, *Polymer*, **15**, 599 (1974).

Received October 25, 1982
Accepted April 19, 1984